energies

MDPI

Article

Recycling Possibility of the Salty Food Waste by Pyrolysis and Water Scrubbing

Ye-Eun Lee [1,2], Jun-Ho Jo [1], Sun-Min Kim [1] and Yeong-Seok Yoo [1,*]

[1] Division of Environment and Plant Engieering, Korea Institute of Civil Engineering and Building Technology 283, Goyang-daero, Ilsanseo-gu Goyang-si, Gyeonggi-do 10223, Korea; yeeunlee@kict.re.kr (Y.-E.L.); junkr@kict.re.kr (J.-H.J.); sunminkim@kict.re.kr (S.-M.K.)

[2] Department of Construction Environment Engineering, University of Science and Technology, 217, Gajeong-ro, Yuseong-gu, Daejeon KS015, Korea

* Correspondence: ysyoo@kict.re.kr; Tel.: +82-31-910-0298; Fax: +82-31-910-0288

Academic Editor: Rafael Luque
Received: 17 November 2016; Accepted: 4 February 2017; Published: 13 February 2017

Abstract: Salty food waste is difficult to manage with previous methods such as composting, anaerobic digestion, and incineration, due to the hindrance of salt and the additional burden to handle high concentrations of organic wastewater produced when raw materials are cleaned. This study presents a possibility of recycling food waste as fuel without the burden of treatment washing with water by pyrolyzing and scrubbing. For this purpose, salty food waste with 3% NaCl was made using 10 materials and pyrolysis was conducted at temperature range between 200–400 °C. The result was drawn from elementary analysis (EA), X-ray photoelectron spectroscopy (XPS) analysis, atomic absorption spectrophotometry (AAS) analysis, water quality analysis and calorific value analysis of char, washed char, and washing water. The result of the EA showed that NaCl in food waste could be volatilized at a low pyrolysis temperature of 200–300 °C and it could be concentrated and fixed in char at a high pyrolysis temperature of 300–400 °C. The XPS analysis result showed that NaCl existed in form of chloride. Through the Na content result of the AAS analysis, NaCl remaining in char after water scrubbing was determined to be less than 2%. As the pyrolysis temperature increased, the chemical oxygen demand (COD) value of scrubbing water decreased rapidly, but the total phosphorus and nitrogen contents decreased gradually. The cleaned pyrolysis char showed an increase of higher heating value (HHV) approximately 3667–9920 J/g due to the removal of salt from the char and, especially at 300–400 °C, showed a similar HHV with normal fossil fuels. In conclusion, salty food waste, which is pyrolyzed at a temperature of 300–400 °C and cleaned by water, can be utilized as high-energy refuse derived fuel (RDF), without adverse effects, due to the volatilization of Cl and an additional process of contaminated water.

Keywords: food waste; NaCl; pyrolysis; X-ray photoelectron spectroscopy (XPS); volatilized; scrubbing; refuse derived fuel (RDF); higher heating value (HHV)

1. Introduction

Food waste can be recycled in various methods, including composting or feed production, heat recovery by combustion, and recovery of methane gas by anaerobic digestion, since it features abundant nutrients, high calorific value and high biodegradation rate [1–4]. Among those, composting and anaerobic digestion are the most commonly used methods [5]. However, it is difficult to recycle salty food waste due to salts. In Korea, food waste represents a large part of municipal solid waste (MSW), approximately 27.4% [6], due to the unique food culture of Korea, but such food waste has high salt content, making it difficult to manage [7].

Salt affects microbial growth, reducing the efficiency of biological treatment, such as composting and anaerobic digestion, and adversely affecting the quality of products, such as compost or feed [8–10]. Incineration also requires salinity treatment beforehand due to the generation of toxic substances or HCI in the combustion reaction [11–13]. Therefore, it is advisable to remove salt from food waste by washing off raw material in order to apply such methods. A large amount of high-concentration organic wastewater is generated in the washing process of salty food waste, creating an additional burden to process such waste.

Therefore, it is necessary to find an alternative to composting, incineration, and anaerobic digestion, in order to process salty food waste effectively. The carbonization of organic waste by pyrolysis increases the binding force of carbon content in organic matter, so it can be an excellent way to reduce the discharge of pollutants in the washing process and utilize char as refuse derived fuel (RDF).

Many studies regarding the carbonization of food waste have been carried out. Li et al. [14] showed that the greatest amount of energy was produced at 250 °C, although a change in carbon content was not significant through the characteristic food waste carbonization products using hydrothermal carbonization at 225 °C, 250 °C, and 275 °C. Parshetti [15] and Han et al. [16] presented a possibility to treat contaminated water with carbonized food waste using the fact that char has an adsorption ability according to the carbonization temperature. Ahmed and Gupta [17] carried out the study regarding syngas, hydrogen gas, and energy recovery through food waste pyrolysis and gasification at the high temperature of 800~900 °C and Liu, Haili, et al. [18] studied the effects of chloride salts contained in food waste on the production of bio-oil and gas through pyrolysis using microwave. Caton et al. [19] focused on dehydration and combustion and discovered that commercial food waste showed high calorific value, indicating a higher possibility of being combustion fuel than a wood pellet. The previous studies mainly focused on an indirect method using food waste char or the recovery of energy in the form of syngas or bio oil, and there was a lack of study to produce and utilize RDF as fuel.

Therefore, this study aimed at improving the quality of fuel by removing salts in char through scrubbing and improving the energy potential using the pyrolysis of food waste.

2. Experimental

2.1. Raw Material

The salty food waste specimen was produced as shown in Table 1 in accordance with Ministry of Environment, Korea [20]. Food waste was classified into grains, vegetables, fruits, meat and fish, and 10 types of raw material were used to have the weight ratio of 16%, 51%, 14%, and 19%, respectively. Salty food waste specimens were ground after 30 g NaCl per 1 kg of food waste was added to adjust the salt concentration to 3% [21,22]. At this time, the salt concentration of specimens was measured and the homogeneity was confirmed by spreading specimens on a 50 cm × 30 cm plate thinly, dividing it into 10 cm × 10 cm sections, and collecting each sample.

Table 1. The standard sample of food waste.

Classification	Composition Ratio (Weight %)	Processing Methods of Food Ingredients	
		Food Ingredients	Processing Method
Grains	16	Rice (16)	
Vegetables	51	Napa cabbage (9) Potato (20) Onion (20) Daikon (2)	Cutting width less than 100 mm. Chop into 5 mm size pieces.
Fruits	14	Apple (7) Mandarin/Orange (7)	Split into 8 pieces in lengthwise.
Meat and Fish	19	Meat (4) Fish (12) Eggshell (3)	Cutting width around 3 cm. Split into 4 pieces.
Total	100	100	

2.2. Method

2.2.1. Experimental Methods

As a lesser weight of pyrolysis char required a lesser amount of water for washing, and the pyrolysis process at a lower temperature required less energy. It was intended to select a section where the highest weight reduction occurred at the lowest temperature. Since a rapid weight reduction of most biomass occurred at a temperature between 200 °C and 400 °C, the temperatures for the experiment were decided to 200 °C, 250 °C, 300 °C, and 400 °C [23]. Figure 1 shows the drawing of the pyrolysis experiment device for this study. It consists of nitrogen feeding entrance, specimen vat, specimen waiting room, pyrolysis furnace, cooler and gas combuster. In order to establish an anaerobic condition in the pyrolysis furnace, nitrogen gas was injected continuously to discharge air inside the furnace. Nitrogen gas was injected from 10 min prior to the insertion of specimens to prevent the oxidation of the specimens. Pyrolysis gas is incinerated in the vent device and discharged to the outside through the fan.

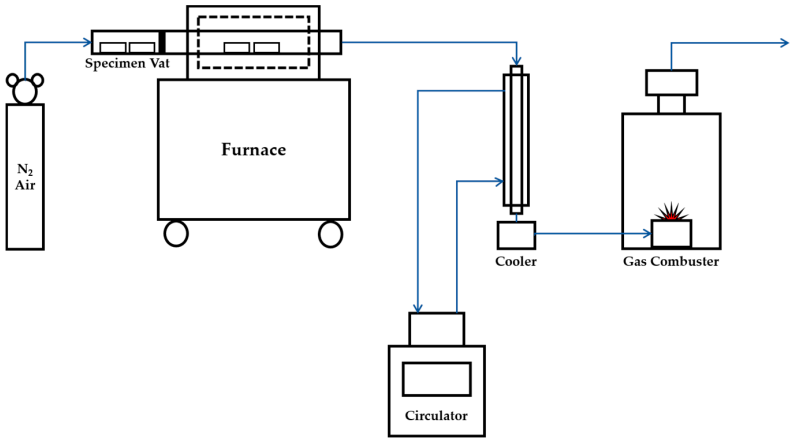

Figure 1. Construction drawing of pyrolysis experiment device.

This experiment was carried out in five stages, including dehydration, pyrolysis, grinding, washing, and dehydration. Two samples were made to compare and confirm the homogeneous. In the dehydration process, the produced standard specimen was dehydrated for 12 h at 105 °C, and its weight was then measured. In the pyrolysis process, the dehydrated specimen was inserted into the pyrolysis device and the pyrolysis process was carried out for two hours at 200 °C, 250 °C, 300 °C, and 400 °C. The specimen was moved and cooled to room temperature. Its weight was measured, and the specimen was then ground. The washing process was carried out in the process in which 10 g of produced char was placed into 100 mL distilled water and stirred for 30 min, and the char and washing water was separated using a filter. The washed char was stored after being dehydrated for 12 h again at 105 °C.

2.2.2. Analytical Methods

The carbonization degree was determined by means of elemental analysis (2400 Series II CHNS/O, PerkinElmer, Boston, MA, USA). Higher heating value (HHV) of carbonization material was measured by a calorimeter (6400 Automatic Isoperibol Calorimeter, Parr, Moline, IL, USA). An atomic absorption spectrometer (AAnalyst400, PerkinElmer, Boston, MA, USA) was used for sodium measurement to determine the sodium chloride content in carbonized food waste. Electron spectroscopy for chemical analysis (K-Alpha, Thermo Fisher Scientific, Tampa, FL, USA) was used to evaluate the relationship between sodium chloride and carbon according to the pyrolysis conditions. All analyses used 1 g of

pyrolyzed char sample that was randomly collected, and each analyses was performed three times, and the whole procedure was performed twice.

In order to determine the pollution level of washing water, a spectrophotometer (DR 5000™ UV-Vis Laboratory Spectrophotometer, HACH, Loveland, CO, USA), nitrogen total low range vial (C-mac), oxygen demand, a chemical (CODcr, C-mac, Daejeon, Korea) high range vial (C-mac, Daejeon, Korea), and a phosphorus total high range vial (C-mac, Daejeon, Korea) were used. The total phosphorus, total nitrogen, and chemical oxygen demand were measured through the dilution and recalculating process.

3. Results and Discussion

3.1. Change of Carbon and Salt According to the Pyrolysis Temperature

Table 2 shows the elementary analysis (EA) result of food waste chars including salt. The correlation R^2 of EA analysis between experimental results is 0.982.

Table 2. Elementary Analysis of pyrolysis chars per temperature.

Temperature	Ultimate Analysis % by Weight						Proximate Analysis % by Weight	Weight Reduction Ratio % by Weight
	C	H	N	S	O	Others	NaCl	
Dried	47.5	12.2	2.9	1.4	29.7	6.3	8.9	33
200 °C	43.2	8.3	3.5	1.3	33.9	9.9	14.6	36.8
250 °C	44.9	8.6	3.6	1.1	30.7	11.1	14.9	38.3
300 °C	47.4	6.1	3.9	1.2	18.7	22.9	20.8	56.9
400 °C	43.1	3.0	2.9	0.9	10.1	39.8	31.7	71.8

The carbon content increases as the pyrolysis temperature increases, then it decreases at 400 °C. Oxygen content and hydrogen content decrease as the pyrolysis temperature increases, and sulfur and nitrogen contents remain constant, unaffected by the pyrolysis temperature. Noncondensable gases such as CO, CO_2, H_2, and CH_4 are the initial product of pyrolysis [24]. Oxygen and hydrogen content decreased due to the volatilization of these initial products by following the pyrolysis process expressed in the below expression:

$$C_nH_mO_p(biomass) \overset{heat}{\rightarrow} \sum_{liquid} C_xH_yO_z + \sum_{gas} C_aH_bO_c + H_2O + C(char). \quad (1)$$

The predicted NaCl value shown in Table 2 shows the salt content in comparison to the whole weight when it is assumed that all 30 g of inserted salt remains after pyrolysis. The weight of the char is 205.43 g, 200.42 g, 144.04 g, and 94.4 g at 200–400 °C, respectively. This value is 4.7%, 3.8% larger at 200 °C, 250 °C and 2.1%, 8.1% smaller at 300 °C, 400 °C in comparison to Others values. In consideration of the fact that the "others" part contains both salt and ash, we can see that the volatilization of salt occurred at 200–250 °C and did not occur at 300–400 °C.

When fossil fuel including Cl is pyrolyzed, it is mostly volatilized at a temperature of 200 °C or higher. If it exists in form of chlorides in the fuel, in other words, the condition of NaCl is in a crystal form due to strong bonding between Na and Cl, it will not be volatilized [25–28]. Additionally, Cl fixed as metal chlorides after pyrolysis when the Cl concentration is high or metal component exists [29,30], and the binding between C and Cl in carbon black which contained approximately 4% to 7% Cl, was rarely found [31]. In the pyrolysis of the driftwood study, Cl emission is reduced when the chlorine is linked with sodium [32]. Collectively, if NaCl content is high, we can expect that the binding between Na and Cl will not break through the pyrolysis. More substances in salty food waste are volatilized into a gas as the pyrolysis is carried out at a higher temperature, while salt is concentrated and remains in a crystal form without being volatilized. This phenomenon can also be confirmed from the X-ray photoelectron spectroscopy (XPS) result.

Figures 2–4 show the C 1s, O 1s, Cl 2p XPS spectra of chars according to the pyrolysis temperature. We can see that a peak moves as the pyrolysis temperature increases. This indicates a chemical transition according to the formation of the compound.

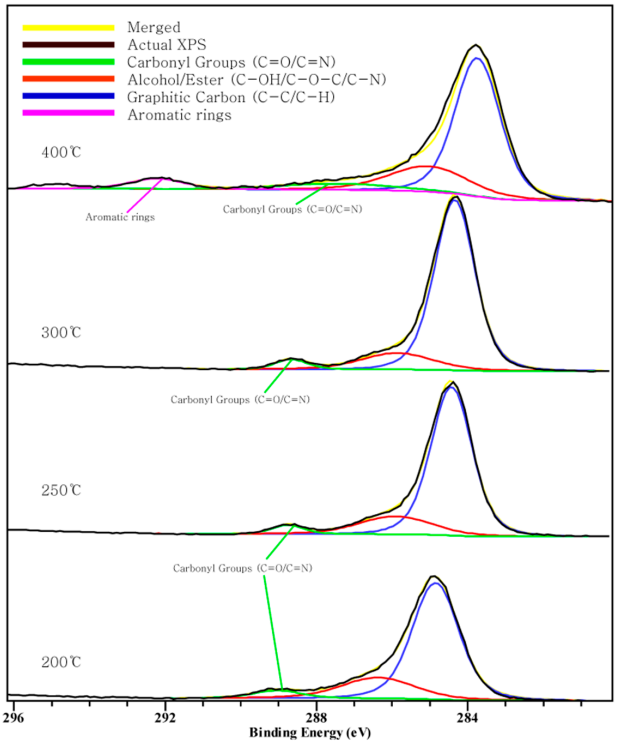

Figure 2. Carbon 1s X-ray photoelectron spectroscopy (XPS) spectra.

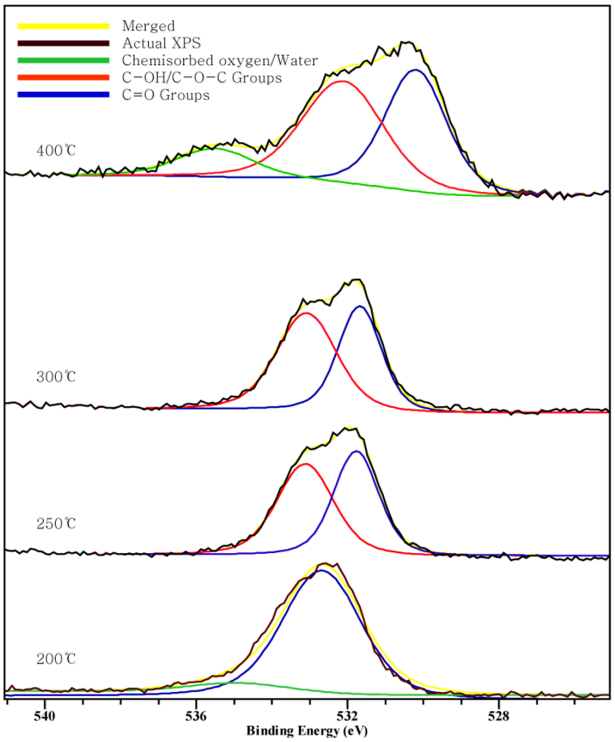

Figure 3. Oxygen 1s XPS spectra.

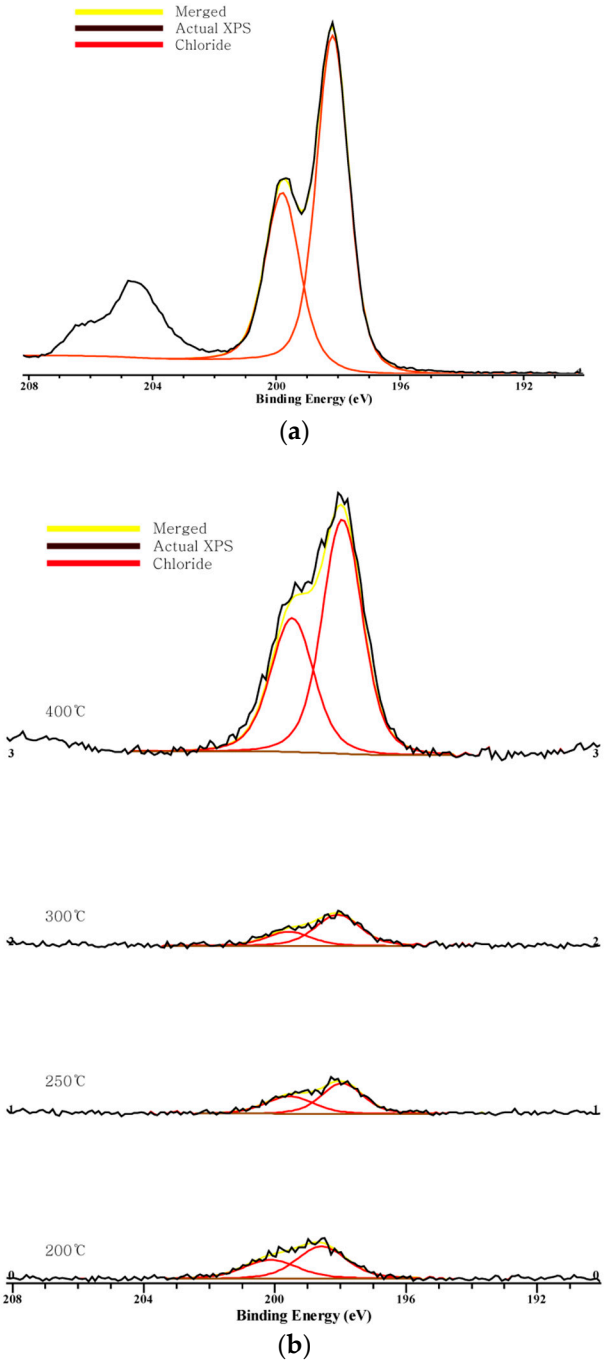

Figure 4. Chlorine 2p XPS spectra: (**a**) NaCl; (**b**) combined.

Three peaks in the C1s spectra. The peak between 284.6–285.1 eV is related to the existence of a C-C/C-H group, and the peak at 289 eV is related to the carboxyl or ester groups. The peak between 291–292 eV indicates the aromatic rings [31,33]. From the C 1s XPS data, the peak between 291–292 eV appeared at 400 °C and the peak at 289 eV appeared at 200~300 °C and disappeared at 400 °C. This indicates some of the carbon forming C-C bonds and forming carboxyl or ester group changing into aromatic carbon. Additionally, the peak at 284.6~285.1 eV moves to the left suggests that there is a connection between the carbon atom and chlorine atom [31]. However, Figure 2 shows the peak moves to the right direction as the pyrolysis temperature increases. That means the carbon is not connected with Cl and another connection exists. The food waste specimen is in a fluidal state, since it

was produced via a grinding method. In this state, NaCl ionized in the food waste water. When the water is vaporized and more heat is added, it seems that sodium and chloride ions combine again. The interaction between Cl and food waste char should be further investigated.

In the O 1s spectra, three peaks at 400 °C and two peaks at 200~300 °C are shown. Three peaks include the peak between 532.4–533.1 eV indicating C-OH or C-O-C groups, a peak at 530.5 eV indicating C=O, and the peak at 535 eV indicating chemisorbed oxygen or water [34]. This result shows that the carboxyl group exists and, as the temperature increases to 400 °C, the amount of oxygen and hydrogen being volatilized and carbon combining with the remaining oxygen in double bonds, through the appearance of C=O carbonyl group, increases.

In the Cl 2p spectra, two peaks are shown near 200 eV and 197.8 eV. The Cl 2p spectra of NaCl also have two peaks at the same positions, and these two peaks indicate chloride. As the peak moves to the left, it suggests the formation of organic Cl [31,35]. The peak moves to the right from 200 °C to 400 °C, implying that binding to chloride rather than binding with organic matter increases, and this can explain the decrease in the amount of volatilized components as the pyrolysis temperature increases. The peak at 200 °C is at 198.7 eV, which is on the left side of the other temperatures, and this indicates that the organic Cl is stronger so that volatilization may occur.

Chlorine shows the peak of chloride and the peak also moves to the right, which means no binding between organic matter and chlorine occurs even if the pyrolysis temperature increases. Carbon also shows its peak moving to the right, and no connection between a carbon atom and a chlorine atom is made. In other words, Cl exists in form of chloride. As the pyrolysis temperature increases and the gasification amount increases, salt is concentrated in the form of chloride and the binding force between Na and Cl increases so that it is not volatilized, even at a high temperature.

3.2. Effects of Pyrolysis Temperature on Salt Washing

Figure 5 shows the analysis results of Na content in salty food waste pyrolysis char and washed char per temperature through atomic absorption spectrophotometry (AAS). The R^2 value of the AAS analysis between the experimental results is 0.935.

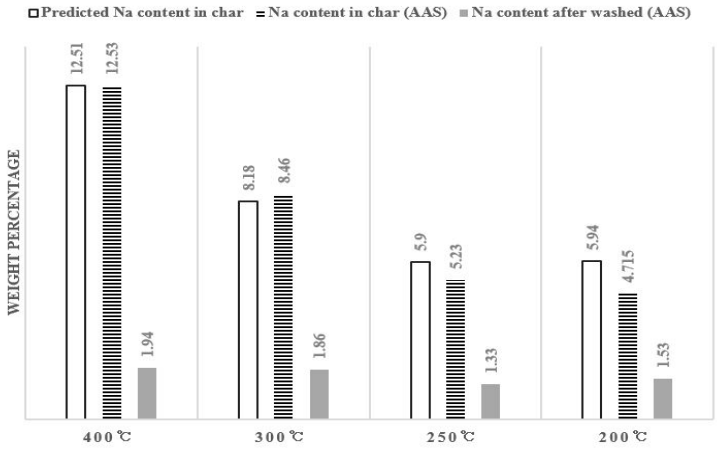

Figure 5. Na content in pyrolysis char (atomic absorption spectrophotometry (AAS) analysis).

The predicted value is calculated by multiplying the predicted salt ratio in Table 2 with the molar mass of Na divided by the molar mass of NaCl. It was assumed that all 30 g of salt remained. The predicted value of Na content and actual Na content before washing are similar and it decreases 12.5% to 5% as the pyrolysis temperature decreases. This is because the ratio of carbon or other substances is higher than that of salt in comparison to the total weight as the pyrolysis temperature decreases as shown in Table 2, not that Na content actually decreases. Around 1% Na remains after washing, although there is a little difference.

The reason for a difference in Na content according to the pyrolysis temperature after washing in Figure 5 is as follows: According to the carbon XPS peak in Figure 2, the peak moves from 284.6–285.1 eV which is the C-C gradually binding to 283 eV of metal carbide as the pyrolysis temperature increases [33,36]. As more Na ions participate such binding, less Na ions will be removed at the time of washing. The data in Figure 3 actually shows that slightly more Na remains in the pyrolyzed residue at a higher temperature after washing than in the pyrolyzed residue at a lower temperature.

Except for the effects of metal carbide, we can see that Na content after water flushing decreases to 1.6% $\pm$ 0.3%. Since salt exists in the form of chloride in the char, it is removed after being ionized in the water. If Na dissolves in water and is removed, Cl also dissolves in water in an ionic state, so we can expect that it will be removed at the same time.

3.3. Effects Pyrolysis Temperature and Salt on the HHV

After washing, the HHV of pyrolyzed specimen increased to 23.7–29.3 KJ/g as the pyrolysis temperature increased. The HHV of the pyrolyzed specimen containing salt increased to 20–22.96 KJ/g to 200–300 °C and it then decreased to 19.4 KJ/g at 400 °C. The predicted value assumes that all 30 g of the salt is removed based on the HHV of the pyrolyzed specimen that contains salt. The predicted value is similar to the HHV value of washed char. The correlation value of HHV analysis shows high repeatability: 0.987.

Figure 6 shows the HHV of the food waste char at each pyrolysis temperature.

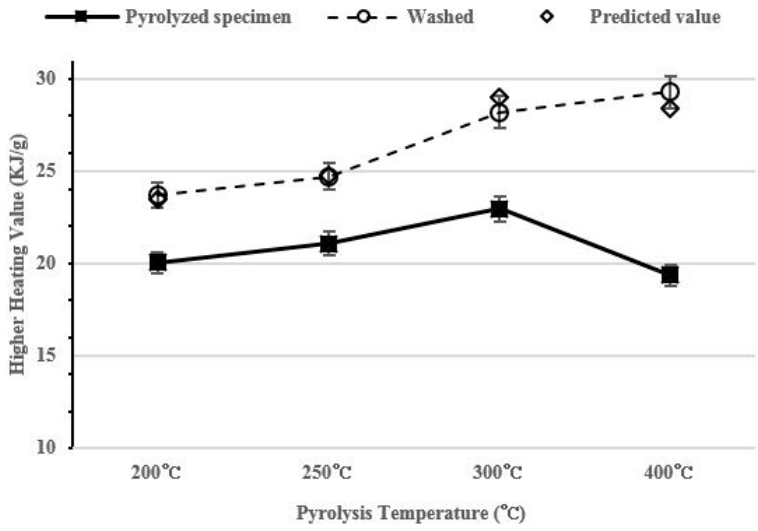

Figure 6. Higher heating value (HHV) per pyrolysis temperature.

As the pyrolysis conducted at a higher temperature, a number of fixed carbon increases and the HHV also increases [37]. Therefore, the highest calorific value should be shown at 400 °C, but the HHV of char before washing tends to decrease. This is because the volume of salt becomes larger than the volume of organic matter in a unit weight while the pyrolysis is being carried out. Compared with the HHV and the result of the elementary analysis in the Table 2, the HHV decreases at the same time when carbon content at 400 °C decreases. Washed char shows a higher HHV as the pyrolysis temperature increases due to the carbon concentration increment and the salt removal. Low-rank coal HHV is about 23~28 KJ/g [38]. Since washed food waste char has 23.7–29.3 KJ/g HHV, the food waste pyrolysis product can be a fossil fuel alternative.

3.4. Change in the Pollution Level of Scrubbing Water

COD, nitrogen, and phosphorus contents were measured in order to check the pollution level of scrubbing water used for removing salt in the food waste pyrolysis char. The graph in Figure 7 shows the total COD, nitrogen and phosphorus contents in washing water diluted by 10 times.

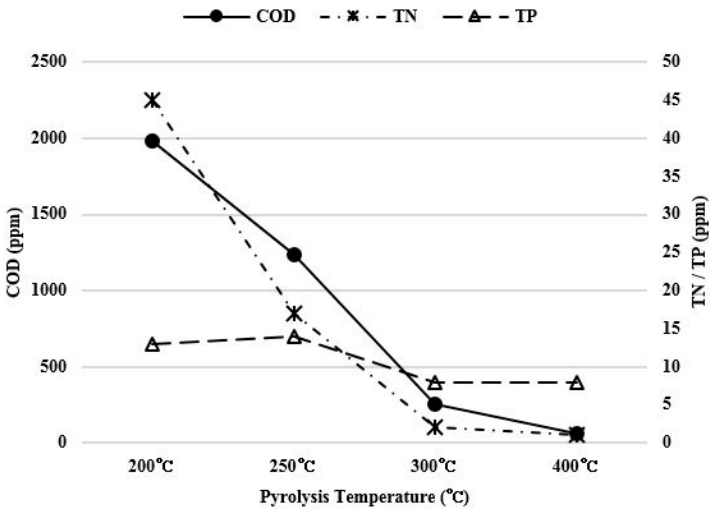

Figure 7. Pollution level of washing water for each pyrolysis temperature.

As the pyrolysis temperature increased from 200 °C to 400 °C, total phosphorus content decreased from 13 ppm to 8 ppm, which was not significant. However, the COD concentration decreased from 1982.5 ppm to 62.5 ppm and the total nitrogen content also decreased from 45 ppm to 1 ppm. The pollution level of the scrubbing water decreased significantly. Especially, a significant COD change occurred because the amount of fixed carbon increased as the pyrolysis temperature increased, and the conversion into aromatic carbon insoluble in water occurred, as shown in Figure 2.

When the pyrolysis temperature increases from 200 °C to 400 °C, the amount of nitrogen existing as a pyrrolic or pyridinic group inside the char increases and the amount of the quaternary nitrogen group decreases [39]. In other words, the nitrogen of the quaternary nitrogen group, such as ammonium ions, change to pyrrolic or pyridinic group. The binding energy of the pyrrolic and pyridinic group are 400.3 ± 0.3 eV, 398.7 ± 0.3 eV, respectively, and the binding energy of quaternary nitrogen, like ammonium ions, is 401.4 eV [40,41]. Figure 8 shows the comparison of N 1s XPS spectra for each pyrolysis temperature. Because the amount of nitrogen in the sample is very low, as shown in Table 2, the peak is scattered. However, the result shows a comparable tendency with Gorbaty and Kelemen et al. [39]. The peak near approximately 401.5 at 200 °C decreases and moves to the right as the temperature increases to 400 °C, and a peak occurs near 398.7 ± 0.3 eV. At 400 °C, the quaternary peak disappeared, and the pyrrolic and pyridinic peaks are clearly indicated. In other words, as the pyrolysis temperature increases, substances, such as ammonium ions, that are easily soluble in water change to the pyridinic groups that are less soluble in water, so the amount of nitrogen that dissolves in scrubbing water is reduced.

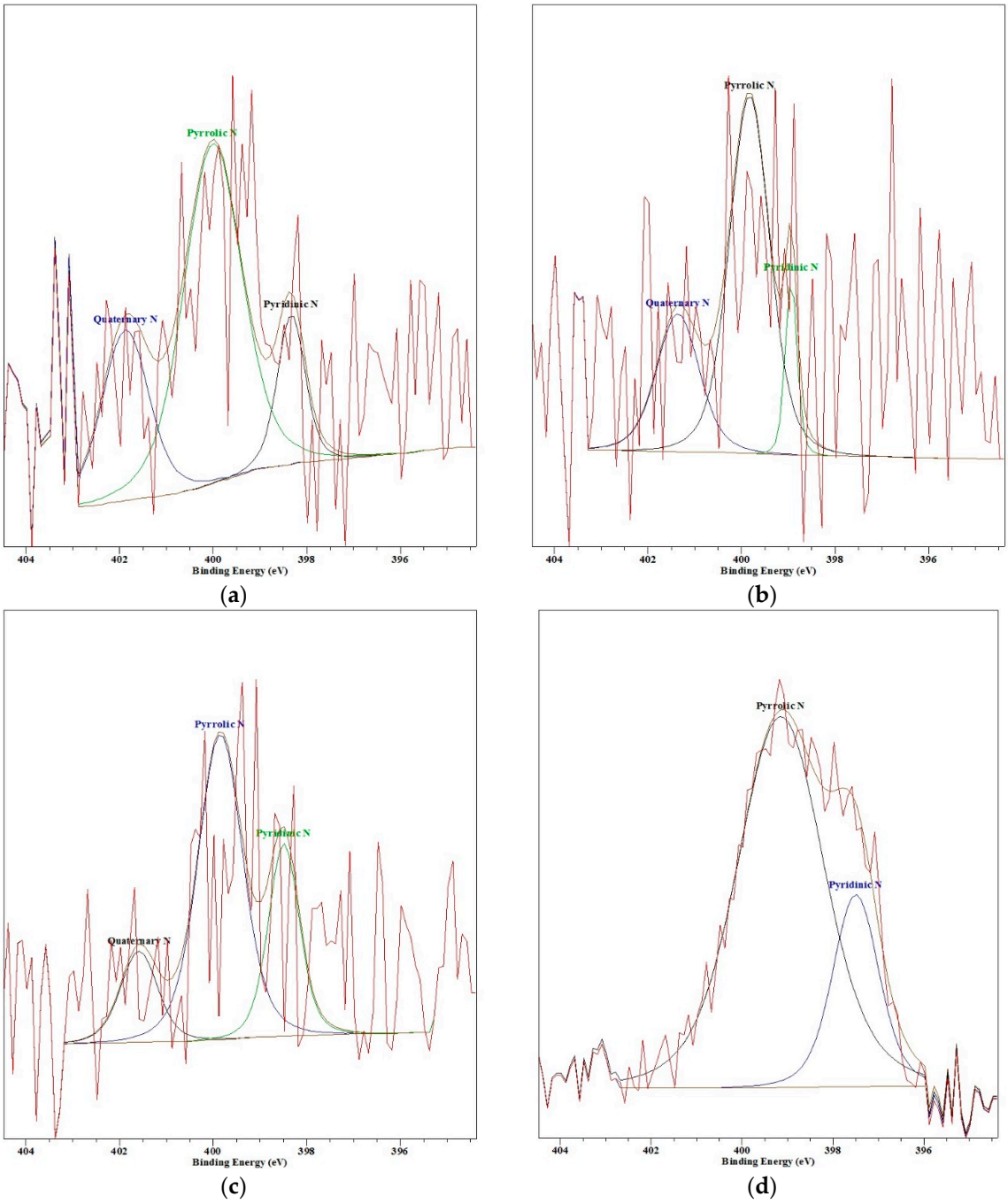

Figure 8. Nitrogen 1s XPS spectra (**a**) 200 °C; (**b**) 250 °C; (**c**) 300 °C; (**d**) 400 °C.

4. Conclusions

This study intended to analyze a possibility of recycling salty food waste as RDF through the pyrolysis of salty food waste and water scrubbing of char.

Salt in fossil fuel is volatilized in the pyrolysis process at a high temperature, but the food waste with high salt content is not volatilized in the pyrolysis process at 300–400 °C. Additionally, salt is concentrated in forms of chloride without combining with organic matters, so it is able to wash out using water.

It was confirmed that as the pyrolysis temperature increased from 200 °C to 400 °C, metal carbide was generated so that the fixed amount of sodium increased from 1.33% to 1.94%, but most of the salt was removed by washing.

The HHV of char at 200–300 °C increases from 20 KJ/g to 22.96 KJ/g but, at 400 °C, decreases to 19.4 KJ/g since the carbon content per unit weight decreases due to salt concentration. The HHV after washing increases to approximately 3.7–10 KJ/g.

The pollution level of scrubbing water decreases since the amount of pollutants being dissolved decreases (the carbon changed 1982.5 to 62.5 ppm, the nitrogen changed 45 to 1 ppm , and the phosphorus changed 13 to 8 ppm) as the pyrolysis temperature increases.

Acknowledgments: This research was supported by a grant (17AUDP-B083704-04) from the Architecture & Urban Development Research Program funded by the Ministry of Land, Infrastructure and Transport of the Korean government.

Author Contributions: Jun-Ho Jo and Yeong-Seok Yoo designed the experiment devices; Jun-Ho Jo and Sun-Min Kim contributed to the analysis of experimental results; Ye-Eun Lee performed the experiments, analyzed the data, and wrote the paper.

Conflicts of Interest: The authors declare no conflicts of interest.

References

1. Büyüksönmez, F. Full-scale VOC emissions from green and food waste windrow composting. *Compost Sci. Util.* **2012**, *20*, 57–62. [CrossRef]
2. Banks, C.J.; Chesshire, M.; Heaven, S.; Arnold, R. Anaerobic digestion of source-segregated domestic food waste: Performance assessment by mass and energy balance. *Bioresour. Technol.* **2011**, *102*, 612–620. [CrossRef] [PubMed]
3. EL-Mashad, H.M.; Zhang, R. Biogas production from co-digestion of dairy manure and food waste. *Bioresour. Technol.* **2010**, *101*, 4021–4028. [CrossRef] [PubMed]
4. Kim, M.-H.; Kim, J.-W. Comparison through a LCA evaluation analysis of food waste disposal options from the perspective of global warming and resource recovery. *Sci. Total Environ.* **2010**, *408*, 3998–4006. [CrossRef] [PubMed]
5. Bernstad, A.; La Cour Jansen, J. Review of comparative LCAs of food waste management systems–current status and potential improvements. *Waste Manag.* **2012**, *32*, 2439–2455. [CrossRef] [PubMed]
6. Ministry of Environment. *The State of Waste Generation and Treatment in 2014*; Ministry of Environment: Sejong City, Korea, 2014.
7. Yun, Y.-S.; Park, J.I.; Suh, M.S.; Park, J.M. Treatment of food wastes using slurry-phase decomposition. *Bioresour. Technol.* **2000**, *73*, 21–27. [CrossRef]
8. Hierholtzer, A.; Akunna, J.C. Modelling sodium inhibition on the anaerobic digestion process. *Water Sci. Technol.* **2012**, *66*, 1565–1573. [CrossRef] [PubMed]
9. Cai, H.; Chen, T.; Liu, H.; Gao, D.; Zheng, G.; Zhang, J. The effect of salinity and porosity of sewage sludge compost on the growth of vegetable seedlings. *Sci. Horticult.* **2010**, *124*, 381–386. [CrossRef]
10. Rengasamy, P. Soil processes affecting crop production in salt-affected soils. *Funct. Plant Biol.* **2010**, *37*, 613–620. [CrossRef]
11. Buekens, A.; Cen, K. Waste incineration, PVC, and dioxins. *J. Mater. Cycles Waste Manag.* **2011**, *13*, 190–197. [CrossRef]
12. Williams, P.T. Dioxins and furans from the incineration of municipal solid waste: An overview. *J. Energy Inst.* **2013**, *78*, 38–48. [CrossRef]
13. Huang, K.; Inoue, K.; Harada, H.; Kawakita, H.; Ohto, K. Leaching behavior of heavy metals with hydrochloric acid from fly ash generated in municipal waste incineration plants. *Trans. Nonferrous Metals Soc. China* **2011**, *21*, 1422–1427. [CrossRef]
14. Li, L.; Diederick, R.; Flora, J.R.V.; Berge, N.D. Hydrothermal carbonization of food waste and associated packaging materials for energy source generation. *Waste Manag.* **2013**, *33*, 2478–2492. [CrossRef] [PubMed]

15. Parshetti, G.K.; Chowdhury, S.; Balasubramanian, R. Hydrothermal conversion of urban food waste to chars for removal of textile dyes from contaminated waters. *Bioresour. Technol.* **2014**, *161*, 310–319. [CrossRef] [PubMed]
16. Han, J.-G.; Lee, J.-Y.; Hong, K.-K.; Lee, J.-Y.; Kim, Y.-W.; Hong, S.-M. Adsorption characteristics of Cu2+ and Zn2+ from aqueous solution using carbonized food waste. *J. Mater. Cycles Waste Manag.* **2010**, *12*, 227–234. [CrossRef]
17. Ahmed, I.I.; Gupta, A.K. Pyrolysis and gasification of food waste: Syngas characteristics and char gasification kinetics. *Appl. Energy* **2010**, *87*, 101–108. [CrossRef]
18. Liu, H.; Ma, X.; Li, L.; Hu, Z.; Guo, P.; Jiang, Y. The catalytic pyrolysis of food waste by microwave heating. *Bioresour. Technol.* **2014**, *166*, 45–50. [CrossRef] [PubMed]
19. Caton, P.A.; Carr, M.A.; Kim, S.S.; Beautyman, M.J. Energy recovery from waste food by combustion or gasification with the potential for regenerative dehydration: A case study. *Energy Convers. Manag.* **2010**, *51*, 1157–1169. [CrossRef]
20. Ministry of Environment (MOE). *A Study on Food Waste Reduction Equipment Guidelines and Quality Standard P*; Ministry of Environment: Sejong City, Korea, 2009.
21. Kim, N.C.; Jang, B.M. Sodium chloride decomposting method in food waste compost using triple salt. *J. Korra* **2004**, *12*, 86–94.
22. Seo, J.Y.; Heo, J.S.; Kim, T.H.; Joo, W.H.; Crohn, D.M. Effect of vermiculite addition on compost produced from Korean food wastes. *Waste Manag.* **2004**, *24*, 981–987. [CrossRef] [PubMed]
23. Raveendran, K.; Ganesh, A.; Khilar, K.C. Pyrolysis characteristics of biomass and biomass components. *Fuel* **1996**, *75*, 987–998. [CrossRef]
24. Basu, P. *Biomass Gasification, Pyrolysis and Torrefaction: Practical Design and Theory*; Academic Press: London, UK, 2013.
25. Quyn, D.M.; Wu, H.; Li, C.-Z. Volatilisation and catalytic effects of alkali and alkaline earth metallic species during the pyrolysis and gasification of Victorian brown coal. Part I. Volatilisation of Na and Cl from a set of NaCl-loaded samples. *Fuel* **2002**, *81*, 143–149. [CrossRef]
26. Quyn, D.M.; Wu, H.; Bhattacharya, S.P.; Li, C.-Z. Volatilisation and catalytic effects of alkali and alkaline earth metallic species during the pyrolysis and gasification of Victorian brown coal. Part II. Effects of chemical form and valence. *Fuel* **2002**, *81*, 151–158. [CrossRef]
27. Wu, H.; Quyn, D.M.; Li, C.-Z. Volatilisation and catalytic effects of alkali and alkaline earth metallic species during the pyrolysis and gasification of Victorian brown coal. Part III. The importance of the interactions between volatiles and char at high temperature. *Fuel* **2002**, *81*, 1033–1039. [CrossRef]
28. Quyn, D.M.; Wu, H.; Hayashi, J.; Li, C.-Z. Volatilisation and catalytic effects of alkali and alkaline earth metallic species during the pyrolysis and gasification of Victorian brown coal. Part IV. Catalytic effects of NaCl and ion-exchangeable Na in coal on char reactivity. *Fuel* **2003**, *82*, 587–593. [CrossRef]
29. Yudovich, Y.E.; Ketris, M.P. Chlorine in coal: A review. *Int. J. Coal Geol.* **2006**, *67*, 127–144. [CrossRef]
30. Nomura, S. Behavior of coal chlorine in cokemaking process. *Int. J. Coal Geol.* **2010**, *83*, 423–429. [CrossRef]
31. Papirer, E.; Lacroix, R.; Donnet, J.-B.; Nansé, G.; Fioux, P. XPS study of the halogenation of carbon black—Part 2. Chlorination. *Carbon* **1995**, *33*, 63–72. [CrossRef]
32. Bartocci, P.; Barbanera, M.; D'Amico, M.; Laranci, P.; Cavalaglio, G.; Gelosia, M.; Ingles, D.; Bidini, G.; Buratti, C.; Cotana, F.; et al. Thermal degradation of driftwood: Determination of the concentration of sodium, calcium, magnesium, chlorine and sulfur containing compounds. *Waste Manag.* **2016**. [CrossRef] [PubMed]
33. Liu, F.-R.; Li, W.; Guo, H.-Q.; Li, B.-Q.; Bai, Z.-Q.; Hu, R.-S. XPS study on the change of carbon-containing groups and sulfur transformation on coal surface. *J. Fuel Chem. Technol.* **2011**, *39*, 81–84.
34. Wang, L.; Shinohara, T.; Zhang, B.-P. XPS study of the surface chemistry on AZ31 and AZ91 magnesium alloys in dilute NaCl solution. *Appl. Surf. Sci.* **2010**, *256*, 5807–5812. [CrossRef]
35. Lu, J.; Luo, M.; Lei, H.; Li, C. Epoxidation of propylene on NaCl-modified silver catalysts with air as the oxidant. *Appl. Catal. A Gen.* **2002**, *237*, 11–19. [CrossRef]
36. Kimmel, Y.C.; Esposito, D.V.; Birkmire, R.W.; Chen, J.G. Effect of surface carbon on the hydrogen evolution reactivity of tungsten carbide (WC) and Pt-modified WC electrocatalysts. *Int. J. Hydrogen Energy* **2012**, *37*, 3019–3024. [CrossRef]

37. Angin, D. Effect of pyrolysis temperature and heating rate on biochar obtained from pyrolysis of safflower seed press cake. *Bioresour. Technol.* **2013**, *128*, 593–597. [CrossRef] [PubMed]
38. Saidur, R.; Abdelaziz, E.A.; Demirbas, A.; Hossain, M.S.; Mekhilef, S. A review on biomass as a fuel for boilers. *Renew. Sustain. Energy Rev.* **2011**, *15*, 2262–2289. [CrossRef]
39. Gorbaty, M.L.; Kelemen, S.R. Characterization and reactivity of organically bound sulfur and nitrogen fossil fuels. *Fuel Process. Technol.* **2001**, *71*, 71–78. [CrossRef]
40. Tian, Y.; Zhang, J.; Zuo, W.; Chen, L.; Cui, Y.; Tan, T. Nitrogen conversion in relation to NH3 and HCN during microwave pyrolysis of sewage sludge. *Environ. Sci. Technol.* **2013**, *47*, 3498–3505. [PubMed]
41. Liu, H.; Zhang, Y.; Li, R.; Sun, X.; Désilets, S.; Abou-Rachid, H.; Jaidann, M.; Lussier, L.S. Structural and morphological control of aligned nitrogen-doped carbon nanotubes. *Carbon* **2010**, *48*, 1498–1507. [CrossRef]